

# Undrained monotonic behavior of sand from self-boring pressuremeter

Debasis Roy

*Klohn-Crippen Consultants Limited, Richmond, B.C., Canada*

Richard G. Campanella & Peter M. Byrne

*University of British Columbia, Vancouver, B.C., Canada*

John Hughes

*Hughes In-Situ Engineering, Inc., Vancouver, B.C., Canada*

**ABSTRACT:** An analytical procedure for estimating undrained stress-strain behavior of sand from drained self-boring pressuremeter tests (SBPMT) data is proposed. Data from two sites have been analyzed using the procedure to predict the mechanical behavior of an axisymmetric element over a wide range of deformation. The results are compared with laboratory triaxial test data on frozen samples to validate the procedure.

## 1 INTRODUCTION

Empirical correlations are available for estimating undrained strength of granular soils from in-situ index tests, e.g., piezocone penetration test (CPTU) or standard penetration test (SPT). However, none of these procedures provides information about how the undrained shear strength develops with increasing deformation. In addition, these relationships do not account for stress, stress path and fabric dependency of mechanical response of granular materials. A procedure has been proposed in this paper to overcome these deficiencies. The procedure is based on calibration of a simple stress strain relationship from SBPMT data and supplementary information from seismic CPT. The calibrated model can be used in deformation analysis of an earth structure.

## 2 MODELING ELASTIC BEHAVIOR

For isotropic elastic material, the strain increment is given by

$$d\varepsilon_{ij}^e = C_{ijkl}^e d\sigma_{kl}' \quad (1)$$

where  $\sigma_{kl}'$  is the effective Cauchy stress and  $D_{ijkl}^e$  is the elastic compliance tensor. The elastic stiffness tensor,

$C_{ijkl}^e$ , is given by

$$C_{ijkl}^e = G_E \left( -\frac{2\nu}{1+\nu} \delta_{ij} \delta_{kl} + \delta_{ik} \delta_{jl} + \delta_{il} \delta_{jk} \right) \quad (2)$$

where  $\delta_{ij}$  represents Kronecker's delta, and  $\nu$  is the Poisson's ratio. The elastic tangent shear modulus,  $G_E$ , for a hyperelastic material can be expressed as (Molenkamp, 1988)

$$G_E = K_{GE} P_A \left[ I_1 / (3 P_A) \right]^{n_E} \quad (3)$$

where  $K_{GE}$  (elastic Shear modulus number) and  $n_E$  (elastic exponent) are model parameters,  $P_A$  is the atmospheric pressure and  $I_1$  (the first invariant) is the trace of the effective stress tensor.

The value of  $n_E$  is about 0.5 for a number of sands. A value of 0.2 can be assumed for  $\nu$  for many sands irrespective of the void ratio. Parameter  $K_{GE}$  mainly depends on soil type and the state of packing. The appropriate in-situ estimate of  $K_{GE}$  can be found from shear wave velocity measurements from seismic CPTU and a reasonable knowledge of in-situ state of stress. To account for the influence of the state of packing on  $G_E$ , the value of  $K_{GE}$  is updated during the deformation process in proportion with  $(2.17-e)^2/(1+e)$ , where  $e$  is the current void ratio.

### 3 MODELING PLASTIC BEHAVIOR

The plastic behavior in distortion is often modeled by adopting a loading surface that has an appearance similar to a cone in the principal stress space with its apex at the origin. Since the conical loading surface opens out along the hydrostatic axis, the distortion mechanism does not predict plastic deformation in isotropic compression. To account for the plastic deformation in isotropic compression, a second loading surface is introduced. For isotropic materials, the loading surface for isotropic compression takes a spherical shape in the principal effective stress space and is sometimes called the "cap". The plasticity mechanisms for distortion and isotropic compression are assumed to be mutually non-interactive and of the strain hardening type.

#### 3.1 Distortional Behavior

We begin with the definition of the Spatial Mobilized Plane (SMP). SMP is defined such that at its intersection with the plane normal to the principal direction "k" of the effective stress tensor, the ratio,  $(\sigma_{(i)}' - \sigma_{(j)}') / (\sigma_{(i)}' + \sigma_{(j)}')$ , is maximized (Nakai and Matsuoka, 1983).  $\sigma_{(i)}'$  are the principal values of  $\sigma_{ij}'$ . The normal ( $\sigma_{SMP}$ ) and the shear ( $\tau_{SMP}$ ) components of the effective stress tensor on this plane and the ratio  $\sigma_{SMP}$  to  $\tau_{SMP}$ ,  $\eta$  (often referred to as the stress ratio), are given by

$$\sigma_{SMP} = 3 I_3 / I_2, \quad \tau_{SMP} = \sqrt{I_1 I_3 / I_2 - 9 I_3^2 / I_2^2} \quad (4)$$

$$\eta = \sqrt{I_1 I_2 / (9 I_3)} - 1$$

The second invariant of effective stress tensor,  $I_2$ , is equal to  $[(\sigma_{kk}')^2 - \sigma_{ij}'\sigma_{ij}'] / 2$  and the third invariant,  $I_3$ , is equal to the determinant of  $\sigma_{ij}'$ . Constant  $\eta$  lines represent the loading surfaces, i.e., yielding occurs when  $\partial\eta / \partial\sigma_{ij}' d\sigma_{ij}' \geq 0$ . Assuming the particles are mobilized to the maximum extent on the average along the SMP, it follows from micro mechanics (Matsuoka, 1974) that

$$\eta = -\lambda (d\epsilon_{SMP} / d\gamma_{SMP}) + \mu \quad (5)$$

where  $d\epsilon_{SMP}$  and  $d\gamma_{SMP}$  are the components of  $d\epsilon_{(i)}^s$

normal and parallel to the SMP.  $d\epsilon_{(i)}^s$ , denotes the principal values of the strain increment of the mechanism for distortional plasticity,  $d\epsilon_{ij}^s$ .  $\lambda$  and  $\mu$  are model parameters. Assuming a hyperbolic relationship between  $\gamma_{SMP}$  and  $\eta$  the instantaneous slope,  $G_{PT}$  ( $= d\eta / d\gamma_{SMP}$ ), can be calculated from (Salgado, 1990)

$$G_{PT} = G_{PI} (1 - R_F \eta / \eta_F)^2 = K_{SP} (\sigma_{SMP} / P_A)^{n_p} (1 - R_F \eta / \eta_F)^2 \quad (6)$$

where  $G_{PI}$  is the initial slope of the  $\eta$ - $\gamma_{SMP}$  curve,  $\eta_{ULT}$  is the asymptotic value of stress ratio as  $\gamma_{SMP}$  increases.  $K_{SP}$ ,  $n_p$  and  $R_F$  are model parameters. The stress ratio at failure,  $\eta_F$ , is assumed to depend on  $I_{1F}$ , the trace of the effective stress tensor at failure, as follows

$$\eta_F = \eta_{F1} - \Delta \eta \log \{ I_{1F} / (3 P_A) \} \quad (7)$$

where  $\eta_{F1}$  and  $\Delta \eta$  are model parameters. From Eqs. (5) and (6)

$$d\epsilon_{SMP} = (\mu - \eta) / (\lambda G_{PT}) d\eta \quad (8)$$

Assuming the principal directions of  $d\epsilon_{ij}^s$  and  $\sigma_{ij}'$  to be the same, the direction cosines of  $d\epsilon_{SMP}$  can be calculated from Eq. (5). Assuming further that  $d\gamma_{SMP}$  and  $\tau_{SMP}$  are coaxial,  $d\epsilon_{(i)}^s$  can be calculated from

$$d\epsilon_{(i)}^s = a_i \{ d\epsilon_{SMP} + d\gamma_{SMP} (\sigma_i' - \sigma_{SMP}) / \tau_{SMP} \} = a_i / G_{PT} \{ (\mu - \eta) / \lambda + (\sigma_i' - \sigma_{SMP}) / \tau_{SMP} \} d\eta \quad (9)$$

where  $a_i$  is the direction cosine of a unit normal to the SMP with respect to the principal axes and is equal to  $[I_3 / (I_2 \sigma_{(i)}')]^{1/2}$ . Differentiating  $\eta$  from Eq. (4) and substituting into Eq. (9), an incremental relationship between the principal strain and the effective stress is obtained. Transformation of the strain increment tensor in the principal stress space,  $d\bar{\epsilon}_{ij}^s (= d\epsilon_{(i)}^s \delta_{ij})$ , to the coordinate axes using  $d\epsilon_{ij}^s = N_{ik} N_{jl} d\bar{\epsilon}_{ij}^s$  yields

$$d\epsilon_{ij}^s = C_{ijkl}^s d\sigma_{kl}' \quad (10)$$

where  $N_{ij}$  is the direction cosine of the principal direction "i" with respect to the j-th coordinate.

Parameters  $\lambda$  and  $\mu$  are not affected by the inherent anisotropy (Nakai and Matsuoka, 1983). Studies also suggest that the quantity  $\eta_F$  may not be significantly

affected by inherent anisotropy (see, e.g., Been and Jefferies, 1985). Thus, Eq. (8) only needs to be modified to capture inherent anisotropy. Following modification to Eq. (6) can thus be proposed

$$G_{PT} = G_{PI} (1 - R_F \eta / \eta_F)^2 \\ = n_A K_{SP} (\sigma_{SMP} / P_A)^{n_p} (1 - R_F \eta / \eta_F)^2 \quad (11)$$

where the multiplier  $n_A$  depends on  $\theta$  (the angle between the depositional direction and the normal to the SMP) and an additional model parameter,  $m_A$ , as follows for  $0^\circ \leq \theta \leq 45^\circ$  (for  $\theta \leq 45^\circ$ ,  $n_A=1$ )

$$n_A = 1 - (m_A - 1) (2 \cos^2 \theta - 1) \quad (12)$$

The value of  $\theta$  is updated at the end of a time step.

### 3.2 Behavior in Isotropic Compression

To evaluate the component of plastic strain,  $d\epsilon_{ij}^c$ , due to isotropic compression, an associated plasticity model proposed by Lade (1977) for isotropic materials is used. The loading surface for this formulation is given by

$$f_c = I_1^2 - 2I_2 = \sigma_{ij}' \sigma_{ij}' \quad (13)$$

The relationship essentially represents a family of spherical surfaces in the effective principal stress space. Section of the loading surfaces for the distortion (AOB) and consolidation mechanisms (AB) in triaxial plane are shown schematically in Figure 1. Abbreviations "TXC" and "TXE" are used to denote triaxial compression and extension, respectively. It can be shown that the plastic strain increment,  $d\epsilon_{ij}^c$ , can be found from

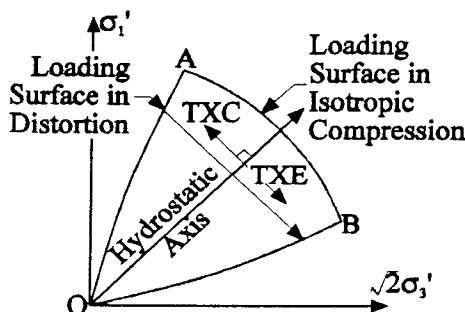


Figure 1. Loading Surfaces

$$d\epsilon_{ij}^c = \frac{C p}{2 f_c P_A} \left( \frac{f_c}{P_A^2} \right)^{p-1} \frac{\partial f_c}{\partial \sigma_{ij}'} \frac{\partial f_c}{\partial \sigma_{kl}'} d\sigma_{kl}' \quad (14)$$

Strain increments from Eqs. (1), (10), (14) are added together to calculate the total strain increment.

### 3.3 Plastic Model Parameters

Two triaxial compression, one triaxial extension, and two isotropic compression on undisturbed samples are needed for calibration of the stress-strain relationship described above. Such an elaborate laboratory testing program is seldom feasible. An approximate calibration procedure in the absence of necessary and sufficient information is outlined below. Information available for calibrating a stress-strain relationship often include data from undrained laboratory element tests on undisturbed samples or in-situ self-boring pressuremeter tests, which are not conventionally used in calibration of constitutive models. These data can be used in a calibration exercise if reasonably precise information about the bounds of values of the model parameters is available. Therefore, existing information on approximate values of model parameters needs to be documented.

**C and p:** Examination of isotropic consolidation tests shows that the parameter, C, is mainly affected by the relative density,  $D_R$ , and grain compressibility. The exponent, p, on the other hand, is affected primarily by grain compressibility only. A relationship is proposed in Figure 2 between parameter C and  $D_R$  that can be used in the absence of more precise information. A value of 0.9 for parameter p appears to be appropriate for granular materials with medium compressibility. The corresponding value for highly compressible soils is 0.65.

Guidelines for selecting approximate values of  $\lambda$ ,  $\mu$ ,  $\eta_{FB}$ ,  $\Delta\eta$ ,  $R_F$ ,  $n_p$  and  $m_A$  from a minimal material specific information are as follows. Once the approximate values of these parameters are identified, model calibration simplifies greatly because iteration over the remaining model parameter,  $K_{SP}$ , is only necessary to fit the model to data.

**$\lambda$  and  $\mu$ :** Nakai and Matsuoka (1983) showed that Eq. (5) does not depend on void ratio or sample fabric and is affected only by soil type. Hence  $\lambda$  and  $\mu$ , can be

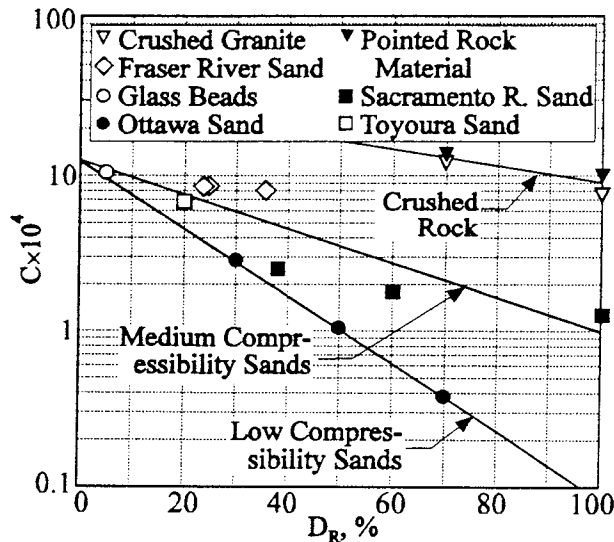


Figure 2. Parameter "C" for Isotropic Compression

evaluated from a suitable drained element test, e.g., triaxial or plane strain, on reconstituted specimens. Typical values of  $\lambda$  and  $\mu$  for many types of sand have been summarized in Roy (1997).

$\eta_{F1}$  and  $\Delta\eta$ : In TXC,  $\eta$  relates to the mobilized effective stress friction angle,  $\phi'$ , by

$$\eta = 2\sqrt{2} \tan \phi' / 3 \quad (15)$$

Since  $(\phi'_F - \phi_{CV})$  relates to the relative density,  $D_R$ , and  $I_{1F}$  (Bolton, 1986),  $\eta_{F1}$  and  $\Delta\eta$  are estimated from a knowledge of  $D_R$ . The relative density of a deposit can be estimated from the cone tip resistance measured in a cone penetration test. Symbols  $\phi'_F$ ,  $I_{1F}$  and  $\phi_{CV}$  denote the values of the effective stress friction angle and  $I_1$  at failure and the steady state friction angle, respectively. Failure is defined as the instance when the peak value of  $\phi'$  is mobilized. The value of  $\phi_{CV}$  is estimated from the knowledge of mineralogy. Estimates of  $\phi_{CV}$  are in fact available in the literature for several types sand (see, e.g., Salgado, 1990; Sasitharan et al., 1994).

The drained angle of internal friction measured in a laboratory element test is usually higher than the corresponding undrained value. Since  $\eta$  relates directly to the peak friction angle in triaxial compression via Eq. (15), model parameters  $\eta_{F1}$  and  $\Delta\eta$  are expected to be depend upon the drainage condition. Examination of a number of laboratory element test data on several sands leads to the following relationship (coefficient of determination

between the two variables,  $R^2 = 0.94$ )

$$(\eta_F - \eta_{CV})_{\text{Undrained}} = 0.46 (\eta_F - \eta_{CV})_{\text{Drained}} \quad (16)$$

The quantity,  $\eta_{CV}$ , is obtained using  $\phi_{CV}$  instead of  $\phi'$  in Eq. (15). Estimates of  $\eta_{F1}$  and  $\Delta\eta$  pertinent to a certain drainage condition can be obtained by modifying the correlation suggested by Bolton according to Eq. (16).

$R_F$  and  $n_p$ :  $R_F$  primarily depends on  $D_R$ . Since the parameter governs the magnitude of irreversible distortion at peak stress ratio, which in turn is not significantly affected by sample fabric and stress path, the effect of stress path and fabric on  $R_F$  is expected to be minimal. Experience with the use of a stress strain relationship similar to that described earlier (Srithar, 1994) appears to indicate that a value of 0.75 is appropriate for  $R_F$  for very dense cohesionless soils and a value near unity for very loose deposits. In the absence of material specific information, for an approximate estimate of  $R_F$ , linear interpolation is used in this study setting  $R_F=1.0$  at  $D_R=0$  and  $R_F=0.75$  at  $D_R=100\%$ . Previous experience also suggests that  $n_p$  ranges between -0.3 and -0.6 for many sands (Salgado, 1990; Srithar, 1992). Roy (1997) could simulate a large number of laboratory triaxial and plane strain tests on several sands using  $n_p=-0.5$ .

$m_A$ : Analysis of a large number of laboratory triaxial tests on undisturbed samples indicates that a value of 2.0 is typical for deposits formed in a hydraulic deposition process such as spigotting of mine tailings or fluvial deposition of channel sands (Roy, 1997).

#### 4 UNDRAINED BEHAVIOR FROM SBPMT

The stiffest and softest cavity expansion test data from self-boring pressuremeter tests at J-Pit (a deposit spigotted Syncrude Sand near Fort McMurray, Alberta) and KIDD # 2 (a Holocene channel deposit of Fraser River Sand near Vancouver, BC) were analyzed as plane strain problem. At these sites  $D_R$  varies between 30 and 65 % and the sand are of medium compressibility. Details of the self-boring pressuremeter testing and the numerical model used in their back-analysis can be found in Roy (1997). The back-analysis procedure involves fitting the model response in cylindrical cavity expansion by varying  $K_{SP}$  manually until a reasonable match between the

computed and observed material response is obtained. Estimates of the other parameters are obtained from seismic measurements and estimates of relative density from seismic piezocone penetration tests performed at adjacent locations and guidelines listed above. The results of back analysis are shown in Figure 3, in which the cavity strain (radial deformation at the cavity wall divided by the original radius of the cavity) is plotted against the corresponding cavity pressure. The depth

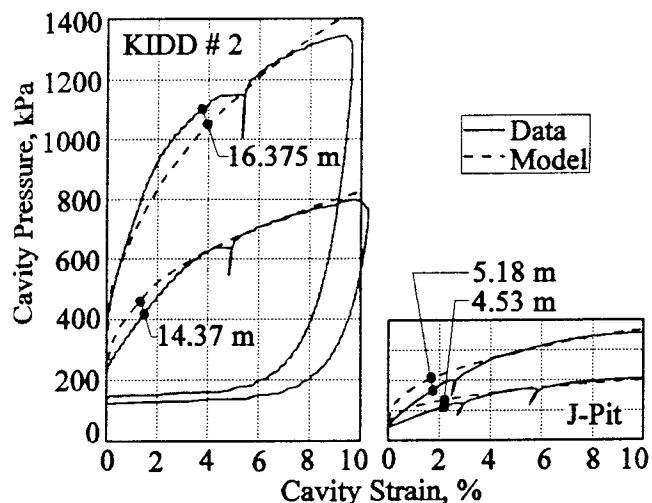


Figure 3. Simulation of SBPMT

of SBPMTs are also indicated in the figure. Model parameters used in back analysis are listed in Table 1. At J-Pit, the effective vertical geostatic stress,  $\sigma_{v_0}'$ , at 4.53 and 5.18 m were taken as 44 and 54 kPa, respectively with a  $K_0$  of 0.5. At KIDD # 2, for the soft layer (14.37 m)  $\sigma_{v_0}'$  and  $K_0$  were taken as 137 kPa and 0.5, respectively. The corresponding values at 16.375 m depth are 155 and 0.7.

Table 1. Model Parameters from SBPMT

Site	$D_R$ %	$K_{GE}$	$\eta_{F1}$	$\Delta\eta$	$K_{SP}$	$R_F$
J-Pit	30	400	0.52	0.01	175	0.98
	60	500	0.62	0.06	1000	0.87
KIDD	30	750	0.71	0.06	240	0.98
	60	1100	0.79	0.10	1000	0.82

Note: For Syncrude Sand,  $\phi_{cv}=28^\circ$ ,  $\lambda=0.85$  and  $\mu=0.29$ . The corresponding values for Fraser River Sand are  $32^\circ$ , 0.77 and 0.39, respectively.

Using the parameters obtained from the back analysis, the undrained triaxial behavior of Syncrude tailings and Fraser River sand is estimated (shown as broken lines in Figure 4). Undisturbed samples were extracted via ground freezing from locations adjacent to the SBPMTs and triaxial compression and extension tests were conducted in the laboratory. Tests on samples with relative density at consolidation,  $D_{RC}$ , similar to those pertaining to the SBPMTs are shown in Figure 4. The samples were anisotropically consolidated to a vertical effective stress,  $\sigma'_{VCONS}$  as shown in Table 2 and a horizontal effective stress ( $\sigma'_{HCONS}$ ) of  $0.5 \times \sigma'_{VCONS}$ . The reasonable agreement between predicted and measured response in Figure 4 suggests that fundamental soil parameters obtained

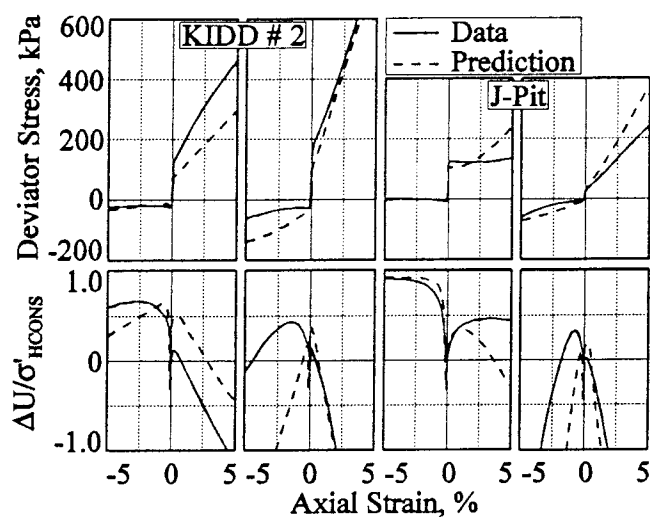


Figure 4. Predicted and Measured Triaxial Stress-Strain Curves ( $\Delta U$  is pore water pressure)

Table 2. Particulars of Triaxial Tests

Site	Test No.	$D_{RC}$ %	$\sigma'_{VCONS}$ kPa	Type
J-Pit	FS5C1B31	31	44	TXE
	FS5C1B32	31	44	TXC
	FS26C211	58	40	TXE
	FS6C2B24	66	48	TXC
KIDD	K94F1C70	67	150	TXE
	K94F1C23	53	120	TXC
	K94F3C4B2	36	156	TXE
	K94F2C2A	40	145	TXC

from pressuremeter tests can be used to estimate undrained element response. The estimated values of the parameters are useful in finite element or finite difference effective stress analysis of static liquefaction problem.

## 5 CONCLUSIONS

A realistic stress-strain model is proposed in this study for frictional materials with inherent anisotropy. Guidelines for the selection of appropriate values of a majority of model parameters are also documented. Necessary and sufficient data are seldom available for calibration of a stress-strain model such as that described in this paper. In such a situation, the constitutive model can be reasonably calibrated utilizing the guidelines and available test data. A procedure is suggested for calibrating the model from self-boring pressuremeter data. The procedure has been validated by comparing the computed triaxial response with model parameters back figured from SBPMTs with the observed laboratory behavior of undisturbed samples. The proposed method based on inverse modeling of SBPMT can be useful in the assessment of static liquefaction potential; a problem in which the traditional empirical procedures based on in-situ tests such as SPT and CPTU have not been very successful.

## ACKNOWLEDGEMENTS

This study was partly funded by the Canadian Liquefaction Experiment (CANLEX), a research undertaking of several educational institutions, industrial participants, and Natural Sciences and Engineering Research Council of Canada (NSERC). The first author also would like to thank the University of British Columbia for financial support through University Graduate Fellowship.

## REFERENCES

- Been, K., and Jefferies M.G. 1985. A state parameter for sands: reply to discussion. *Géotechnique*, 35, 127-132.
- Bolton, M.D. 1986. The strength and dilatancy of sands. *Géotechnique*, 36, 65-78.
- Lade, P.V. 1977. Elasto-plastic stress-strain theory for cohesionless soil with curved yield surfaces. *Int. J. of Solids and Structures*, London, 13, 1019-1035.
- Lade, P.V., and Nelson, R.B. 1987. Modelling the elastic behaviour of granular materials. *Int. J. for Numerical and Analytical Methods in Geomechanics*, 11, 521-542.
- Matsuoka, H. 1974. A microscopic study on shear mechanisms of granular materials. *Soils and Foundations*, 14(1), 29-43.
- Molenkamp, F. 1988. A simple model for isotropic non-linear elasticity for friction materials. *Int. J. for Numerical and Analytical Methods in Geomechanics*, 12, 467-475.
- Nakai, T., and Matsuoka, H. 1983. Shear behaviors of sand and clay under three-dimensional stress condition. *Soils and Foundations*, 23(2), 26-42.
- Roy, D. 1997. Deformation behavior of granular deposits from self-boring pressuremeter, *Ph.D. Dissertation* (under preparation), Department of Civil Engineering, University of British Columbia, Vancouver.
- Salgado, F.M. 1990. Analysis procedures for caisson-retained island type structures. *Ph.D. Dissertation*, Department of Civil Engineering, University of British Columbia, Vancouver.
- Sasitharan, S., Robertson, P.K., Sego, D.C., and Morgenstern, N. R. 1994. State-boundary surface for very loose sand and its practical implications. *Canadian Geotech. J.*, 31, 321-334.
- Srithar, T. 1994. Elasto-plastic deformation and flow analysis in oil sand masses. *Ph.D. Dissertation*, Department of Civil Engineering, University of British Columbia, Vancouver.
- Stark, T.D., and Mesri, G. 1992. Undrained shear strength of liquefied sands for stability analysis. *J. of Geotech. Engrg.*, ASCE, 118, 1727-1747.